Variations in the light absorption coefficients of phytoplankton, non-algal particles and dissolved organic matter in reservoirs across China

Yingxin Shang[1, 3,5], Pierre-Andre Jacinthe[2], Lin Li[2], Zhidan Wen[1,3], Ge Liu[1,3], Lili Lyu[1, 5], Chong Fang[1,5], Bai Zhang[1,3], Junbin Hou[1], Kaishan Song[1, 3,4*]

[1] Northeast Institute of Geography and Agroecology, CAS, Changchun, 130102, Jilin, China.

[2] Department of Earth Sciences, Indiana University–Purdue University, Indianapolis, IN, USA.

[3]Changchun Jingyuetan Remote Sensing Observation Station, Chinese Academy of Sciences, Changchun 130102, China

[4] School of Environment and Planning, Liaocheng University, Liaocheng, 252000, China

[5] University of Chinese Academy of Science, Beijing, 100049, China.

Corresponding author: Kaishan Song (songkaishan@iga.ac.cn)

Key Points:

- Absorption parameters varied significantly from different regions and trophic states
- Factors affecting the three inherent optical absorption for large-scale regions were explored
- Dominant absorption types for various regions were determined

---

This is the author's manuscript of the article published in final edited form as:

Shang, Y., Jacinthe, P.-A., Li, L., Wen, Z., Liu, G., Lyu, L., Fang, C., Zhang, B., Hou, J., & Song, K. (2021). Variations in the light absorption coefficients of phytoplankton, non-algal particles and dissolved organic matter in reservoirs across China. Environmental Research, 201, 111579. https://doi.org/10.1016/j.envres.2021.111579

Abstract

Reservoirs were critical sources of drinking water for many large cities around the world, but progress in the development of large-scale monitoring protocols to obtain timely information about water quality had been hampered by the complex nature of inland waters and the various optical conditions exhibited by these aquatic ecosystems. In this study, we systematically investigated the absorption coefficient of different optically-active constituents (OACs) in 120 reservoirs of different trophic states across five eco-regions in China. The relationships were found between phytoplankton absorption coefficient at 675 nm ($a_{ph}(675)$) and Chlorophyll a(*Chla*) concentration in different regions (R^2:0.60-0.82). The non-algal particle (NAP) absorption coefficient (a_{NAP}) showed an increasing trend for reservoirs with trophic states. Significant correlation ($p<0.05$) was observed between chromophoric dissolved organic matter (CDOM) absorption and water chemical parameters. The influencing factors for contributing the relative proportion of OACs absorption including the hydrological factors and water quality factors were analyzed. The non-water absorption budget from our data showed the variations of the dominant absorption types which underscored the need to develop and parameterize region-specific bio-optical models for large-scale assessment in water reservoirs.

1 Introduction

The OACs (optically-active constituents) in inland waters typically included phytoplankton, NAP and CDOM (Ylöstalo et al., 2014). The inherent optical properties (IOPs) of OACs in water bodies were depend on the medium and independent of the ambient light field, so that underwater light absorption coefficients of OACs can be used to investigate the variability of OACs in natural waters under various aquatic and environmental conditions (Lyu et al., 2020, Matsuoka et al., 2011). The complexity of sources and composition of OACs enhance the variability of optical properties of Case-2 waters, including inland water reservoirs (Li et al., 2017, Wu et al., 2011). Reservoirs were constructed to meet a variety of needs, including irrigation, recreation and drinking water storage, and consequently contribute to the survival and well-being of human communities. Water quality in reservoirs can be a challenge, thus creating the need to establish monitoring programs that are flexible, reliable and cost-effective, and can deliver timely information about water quality status (Shi et al., 2019a). According to our comparisons of optical absorption coefficients of reservoirs and lakes across five eco-regions based on in situ field sampling dataset, the mean optical coefficients at 440nm including CDOM, phytoplankton and non-algal particulates for reservoirs are significant higher that of reservoirs ($p<0.05$) (Table S1). There was great interest in understanding light absorption process of OACs of reservoirs in order to develop water quality monitoring programs that provide accurate information about *in-situ* conditions and ensure a safe water supply (Shang et al., 2021).

The *in situ* study for the linkage of optical absorption and water quality parameters was useful to identify the quality and quantity of the components and further calibrated and validated remote sensing models of water quality parameters (Gholizadeh et al., 2016; Zhao et al., 2017).

Phytoplankton absorption coefficients have been related to phytoplankton biomass and *Chla* (Binding et al., 2008). NAP generally consisted of sediments, non-algal organic detritus and living non-algal particulates (Binding et al., 2008). The CDOM also affected the optical properties of aquatic systems through control of UV and blue radiation penetration the water column (Organelli et al., 2016). CDOM was generally derived from autochthonous and allochthonous sources (Jones et al., 2009). Generally, CDOM absorption coefficients at 355nm and 440nm was chosen to represent the relative absorption concentration, and used as CDOM absorption parameters to build remote sensing retrieval for inland waters (Brezonik et al., 2015). Except for absorption coefficient, the absorption slope can provide information about the source and composition of CDOM (Helms et al., 2008; Zhang et al., 2011).

The specific absorption coefficients of OACs could reflect regional variability in inherent optical characteristics of aquatic systems as well as their ecological conditions and trophic state (Shi et al., 2019b; Shang et al., 2019). The specific phytoplankton absorption coefficients can significantly vary among the IOPs of various substances in aquatic systems (Wan et al., 2020; Bricaud et al., 2010; Sun et al., 2012). The intensity and variability of light absorption can be related to the trophic state of a water body since the average size of phytoplankton cells usually increases from oligotrophic to eutrophic waters (Shi et al., 2019b; Ciotti et al., 2002). Investigations into the specific absorption coefficient of NAP have also shown that this parameter varies with region and season (Sun et al., 2012; Tilstone et al., 2012; Astoreca et al., 2012). Particle sizes and composition were key factors determining the optical absorption and scattering characteristics of NAPs in areas such as coastal waters, continental shelves, and semi-arid regions (Binding et al., 2005; Wen et al., 2016). Previous studies have shown that absorption slopes can vary widely depending on the eco-region of the water body investigated, with high slopes of CDOM generally observed in water bodies from high-elevation regions likely due to strong photo-chemical processes (Brito et al., 2015; Babin et al., 2003; Zhang et al., 2011). Due to the complex composition of OACs encountered in reservoirs of inland waters, and the variable hydrological (reservoir's storage) and geomorphological environments present in these waterbodies, light absorption characteristics vary significantly (Li et al., 2012; Vantrepotte et al., 2012).

In many countries around the world, including China, reservoirs account for a significant part of inland waters. As reservoirs are often primary sources for agricultural, urban and industrial uses, they are critical for economic and social development. Previous studies addressing these limitations have generally focused on one reservoirs; consequently, results of these past studies lack regional perspectives and were inadequate to provide a wider view on the variability of OACs across eco-regions (Li et al., 2012; Naik et al., 2013; Shi et al., 2013). According to the Ecological Environment Bulletin in 2017 from Ministry of Ecology and Environment of the People's Republic of China, 23% of the monitoring lakes or reservoirs were eutrophic and 67% of the monitoring important reservoirs or lakes were mesotrophic. Therefore, a comprehensive study of light absorption characteristics in reservoirs spanning across several eco-regions and trophic states would be needed to provide the foundation for water quality monitoring using optical models. The objectives of this study were to: (1) examine the spatial variation of OAC absorption with respect to eco-region and trophic state of water reservoirs; (2) analyze the factors affecting the three inherent optical absorption for large-scale regions were explored; and (3) the dominant absorption types for various regions were determined

2 Materials and Methods

2.1 Study Area

Reservoirs as important drinking water sources according to the list from the Ministry of Ecology and Environment of China were selected to represent the diversity of geographical locations, morphological characteristics, ecological conditions and water uses. For this study, we selected 120 reservoirs distributed across five regions in China. Regions were defined on the basis of variation in hydrological and geological conditions (Zhao et al., 2010), and included: the Northeast hydrological region (NLR), the Eastern hydrological region (ELR), the Yungui plateau hydrological region (YGR), the Mengxin hydrological region (MXR) and the Tibetan Plateau hydrological region (TPR) (Fig. 1). Reservoirs ($>10^4$ m^3) as important drinking water sources across China were selected to represent the diversity of geographical locations, morphological characteristics, ecological conditions and water uses. Accessibility was an additional factor considered in the selection of water reservoirs for this study. All the reservoirs selected were relatively large and representative of the five regions described above.

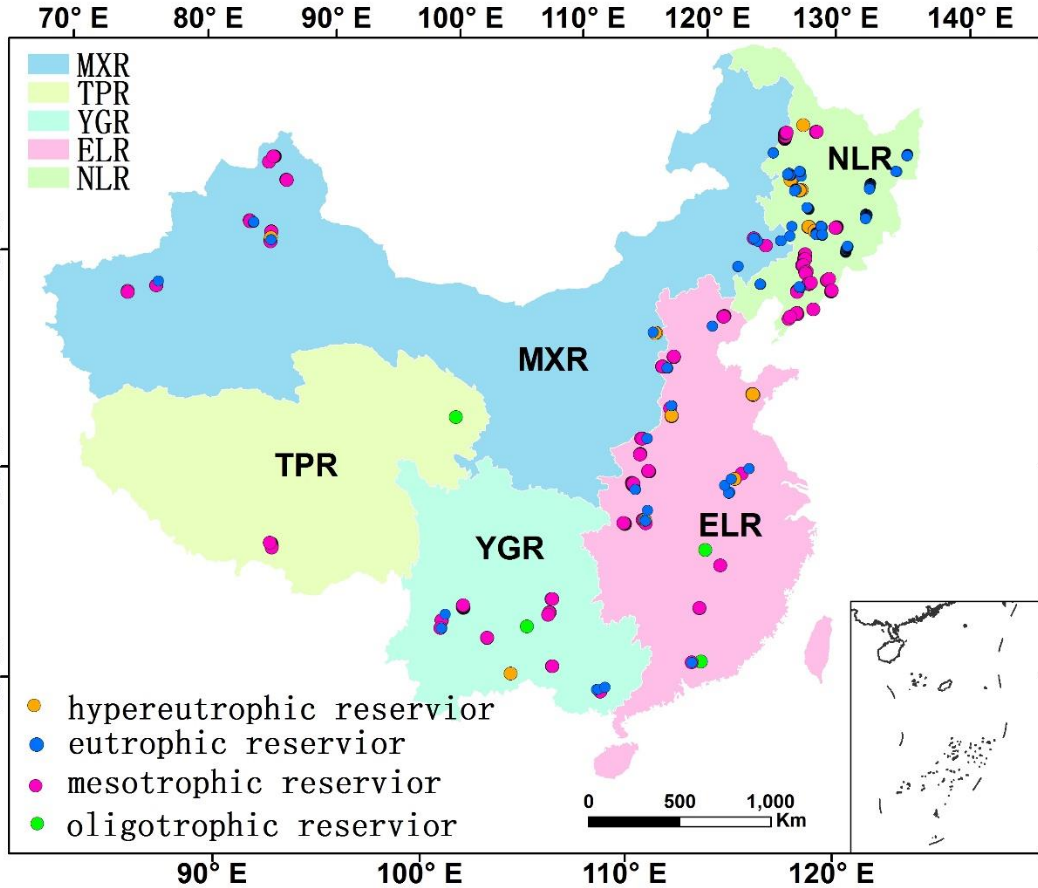

Figure 1 The distribution of sampling reservoirs and main regions across China.

2.2 Sampling description

A total of 507 water samples were collected from 120 reservoirs (3-5 samples in each reservoir; Fig.1) across the five regions of China in autumn between 2014 and 2015 with the consideration of diversity of geographical locations, morphological characteristics, ecological conditions and water uses. Sampled reservoirs exhibit a range of trophic states. Due to the uneven distribution of numbers of reservoirs among regions and the convenience of taking fieldtrips, more water samples was collected in the NLR (40 reservoirs) and ELR regions (39 reservoirs) than in the TPR (3 reservoirs), YGR (17 reservoirs) and MXR regions (21 reservoirs). Water samples were generally collected from the central part of the reservoir. Surface water samples (0.5 m) were collected in 1 L acid-washed plastic bottles, transported in a portable refrigerator, and filtered within 24 h upon returning to the laboratory. Water quality parameters such as temperature, dissolved oxygen, salinity, pH, turbidity, ORP, *Chla*, fluorescent colored dissolved organic matter were measured using in-situ multi-parameter probes (YSI 600 XLM Sonde, YSI Inc., Yellow Springs, OH). Secchi disk depth (SDD) was measured with a Secchi disk.

2.3 Laboratory Measurements

Water samples were initially filtered through a 0.45 μm cellulose acetate micro-porous membrane filter (Peninsula). Dissolved organic carbon (DOC) concentration of water samples was determined using a Shimadzu TOC-5000 analyzer. The concentration of *Chla* was determined by analyzing the absorption spectra of samples extracted with 90% acetone for 24 h at 4 °C using a Shimadzu UV-2600PC spectrophotometer (Shang et al., 2019). To determine the concentration of total solid matter (TSM), water samples were filtered through pre-weighed 47 mm, 0.7 μm pore size glass fiber filters which were then oven dried at 85 °C for at least two hours before cooling and re-weighing. The filters were again heated in a muffle furnace at 400 °C for two hours (Wen et al., 2016) to determine the concentration of MSS (mineral suspended solids) by re-weighing the filters after ignition. Total phosphorus (TP) were measured after oxidation in the presence of boric acid and sodium hydroxide with a standard procedure (APHA/AWWA/WEF, 1998).

2.4 OACs absorption measurements

CDOM was extracted by filtering water samples through a 0.22 μm polycarbonate membrane (Whatman, 110606). The detailed measurement of CDOM spectra and the coefficient calculation process is shown in the supplementary materials. The spectral slopes (S_{CDOM}280-400 and S_{CDOM}275-295) were determined from least- squares regression of log-transformed absorption coefficients in the ranges 280-400 nm and 275-295 nm (Binding et al., 2008; Helms et al. 2008; Song et al., 2010). The specific CDOM absorption at 355nm (a^*_{CDOM}) which was calculated by a_{CDOM}(355) normalized to DOC concentration was obtained as well.

Total particulate absorption coefficients (ap) were determined using the quantitative filter technique (QFT) (Mitchel et al., 2002). Water samples were filtered through 0.7 μm pore size Whatman GF/FTM filters before measuring the absorption coefficients of total particulate absorption (ap(λ)). Non-algal particulate absorption ($a_{NAP}(\lambda)$) was obtained using the methanol extraction method to remove pigment matter. The spectral absorption coefficient for NAP was computed (Babin et al., 2003). The phytoplankton absorption coefficient was then obtained as the difference between a_p and $a_{NAP..}$ The spectral slope of the a_{NAP} (S_{NAP})was related to particle size and the relative proportion of mineral and organic particles (Binding et al., 2008). The a^*_{NAP} was calculated with the ratio of a_{NAP} and MSS (Babin & Stramski, 2004). The specific absorption (a^*_{ph}) was calculated with the ratio of a_{ph} and *Chla* concentrations (We use 440nm and 675nm) (Bricaud et al., 1995). The detailed calculation of the particulate absorption is shown in supplementary materials.

Total non-water absorption refered to the total absorption of CDOM, phytoplankton and non-algal particulates (Wen et al., 2016). The relative contribution ratio of the three sources of absorption was calculated with the light absorption coefficient at 440nm normalized to the total non-water absorption at 440nm in this study (Li et al., 2015; Wen et al., 2016). The detailed measurement steps were shown in the supplementary materials.

2.5 Trophic states assessment

Trophic state assessment of the reservoirs was based on the modified Carlson's trophic state index (TSI_M) (Zhang et al., 2018; Lyu et al., 2020, Aizaki, 1981). This index was calculated using three limnological parameters, chlorophyll a (*Chla*, μg/L), Secchi disk transparency (SDD, m) and total phosphorus (TP, μg/L), according to the following equations:

$$TSI_M(Chla) = 10(2.46 + \frac{\ln Chla}{\ln 2.5}) \tag{4}$$

$$TSI_M(SDD) = 10(2.46 + \frac{3.69 - 1.53 \ln SDD}{\ln 2.5}) \tag{5}$$

$$TSI_M(TP) = 10(2.46 + \frac{6.71 + 1.15 \ln TP}{\ln 2.5}) \tag{6}$$

Comprehensive TSI (TSI_M) was calculated with the mean index of the three parameters, 0.297 for SDD, 0.54 for *Chla* and 0.163 for TP. Results from this calculation range from 0 to 100 and provide a scale to rate the trophic state of the reservoirs: $0<TSI_M \leq 30$ oligotrophic; $30<TSI_M \leq 50$ mesotrophic; $TSI_M > 50$ eutrophic (Shang et al., 2019), among the eutrophic states, the index larger than 70 was considered as hypereutrophic states.

2.6 Hydrological dataset collection

The hydrological dataset including design flood level (the highest water level in a reservoir after flooding), total storage, flood regulation storage capacity, normal pool level, spillway design flood level, beneficial reservoir capacity, flood limit level, inactive storage capacity (the lowest water level under normal operation of a reservoir), dead water level for main reservoirs was purchased from the local hydrographic offices and the data was used to analyze the influences of hydrological factors on OACs properties.

2.7 Data analysis

The variability of OACs properties in water reservoirs from different regions and trophic states was examined, and statistical analyses (mean value, standard deviation, linear or non-linear regression, t-test) were conducted using SPSS 22.0 (SPSS, Chicago, IL, USA). K-means clustering analysis was used to evaluate the water classification types based on light absorption coefficients (Spyrakos et al., 2017). Correlation plots of different OACs-related parameters were constructed using Origin 9.0 (Origin Lab, Northampton, MA). Spatial distribution of sampling sites was conducted using ArcGIS 10.1 software. Difference among water reservoirs in regard to OACs indices was assessed with one-way ANOVA. Statistically significant difference was determined at $p<0.01$.

3 Results

3.1 Biogeochemical parameters

For some of the water quality parameters used for trophic state assessment, mean values can increase by an order of magnitude between oligotrophic and hyper eutrophic reservoirs (Table 1). The temperature ranged from 10.8 to 22.5℃. No significant difference was observed among regions ($p>0.05$). There were significant differences between reservoirs in the MXR and YGR regions in regard to DOC concentration ($p<0.05$). TSM concentration ranged from 0.17 to 478.50 mg/L for reservoirs across regions (Table 2). *Chla* concentration ranged from 0.04 to 3380.45 μg/m^3 for different trophic states. *Chla* concentration in different hydrological regions was different ($p<0.05$). *Chla* in reservoirs from the ELR, MXR and NLR regions was significantly higher than in those from the TPR and YGR regions. Overall, water chemistry parameters in NLR, ELR and MXR water reservoirs were relatively higher than in those from the TPR and YGR regions.

Table 1. Water chemical parameters of different trophic reservoirs

	Oligotrophic (n=4)			Mesotrophic (n=50)			Eutrophic (n=54)			Hyper Eutrophic (n=12)		
	Mean	Min.	Max.	Mean	Min.	Max.	Mean	Min.	Max.	Mean	Min.	Max.
TSM(mg/L)	0.46	0.01	1.80	3.93	0.17	478.50	25.24	1.50	184.00	48.6	14.40	310.00
SDD (m)	5.74	5.08	11.30	2.03	0.36	3.28	0.59	0.01	2.99	0.24	0.10	0.48
Chla (μg/L)	0.33	0.04	1.40	3.81	0.00	107.51	21.65	0.00	61.83	106.03	2.80	3380.45
DOC(mg/L)	2.04	0.67	2.94	2.93	0.70	22.62	8.49	0.91	60.60	10.9	4.03	71.04
TP (mg/L)	0.001	0.0008	0.02	0.03	0.002	0.11	0.06	0.01	1.65	0.58	0.01	10.37

Note: TSM=concentration of total solid matter, DOC=dissolved organic carbon, SDD=Secchi disk depth, *Chla*=chlorophyll-a concentration; TP=Total Phosphorus; *N*=numbers of reservoirs

Table 2 The mean water chemistry parameters for reservoirs in five lake regions.

	NLR		ELR		MXR		TPR		YGR	
	Mean	Min-Max	Mean	Min-Max	Mean	Min-Max	Mean	Min-Max	Mean	Min-Max
TSM(mg/L)	25.79	0.17-478.50	9.92	0.2-310.0	25.28	2.33-134.54	1.01	0.01-4.50	3.53	0.20-19.00
SDD(m)	0.93	0.01-4.32	4.94	0.16-6.80	0.77	0.25-1.70	6.71	3.08-11.30	1.98	0.40-5.80
Chla(μg/L)	22.40	1.02-219.70	46.71	0.31-3380.5	15.63	0.17-213.88	0.41	0.041-1.40	6.91	0.38-22.07
DOC (mg/L)	6.44	0.98-33.56	3.97	0.70-71.04	9.87	1.12-60.60	5.22	1.94-9.46	1.90	0.76-6.29
TP(mg/L)	0.07	0.006-0.833	0.22	0.001-10.37	0.04	0.008-0.108	0.04	0.008-0.114	0.004	0.001-0.015

Note: TSM=concentration of total solid matter, DOC=dissolved organic carbon, SDD=Secchi disk depth, *Chl-a*=chlorophyll-a concentration; TP=Total Phosphorus;

3.2 Phytoplankton absorption

Across five regions, the average $a_{ph}(440)$ ranged from 0.174 m^{-1} to 1.53 m^{-1}, and the average $a_{ph}(675)$ ranged from 0.103 m^{-1} to 0.83 m^{-1} (Fig. 2a). With respect to $a_{ph}(440)$, there were significant differences ($p<0.01$) between the YGR (NLR) and MXR regions, and also between trophic states ($p<0.01$). From oligotrophic to hyper eutrophic reservoirs, the average value for $a_{ph}(440)$ ranged from 0.31 m^{-1} to 4.54 m^{-1}, and $a_{ph}(675)$ ranged from 0.18 m^{-1} to 2.54 m^{-1} (Fig. 2b). In the ELR, YGR and NLR regions, strong relationships (R^2: 0.73-0.82) were found between phytoplankton absorption coefficient at 675 nm and *Chla* concentration (Fig.3). However, relationships between these variables were weaker (R^2: 0.60-0.68) in the TPR and MXR regions. The value of a^*_{ph} (440) for various regions and trophic states was shown in Fig.S1.

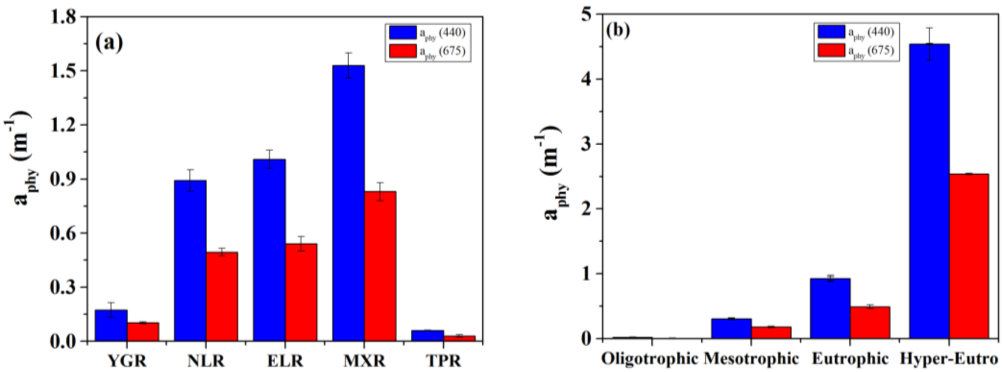

Fig.2 (a) Phytoplankton absorption at 440nm and 675 nm for different lake regions and (b) Comparison for a_{ph} for different trophic status.

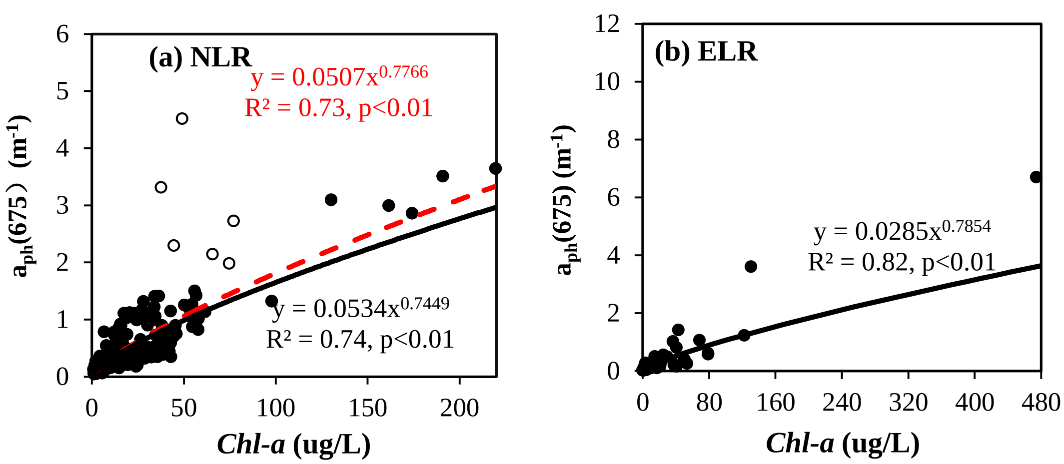

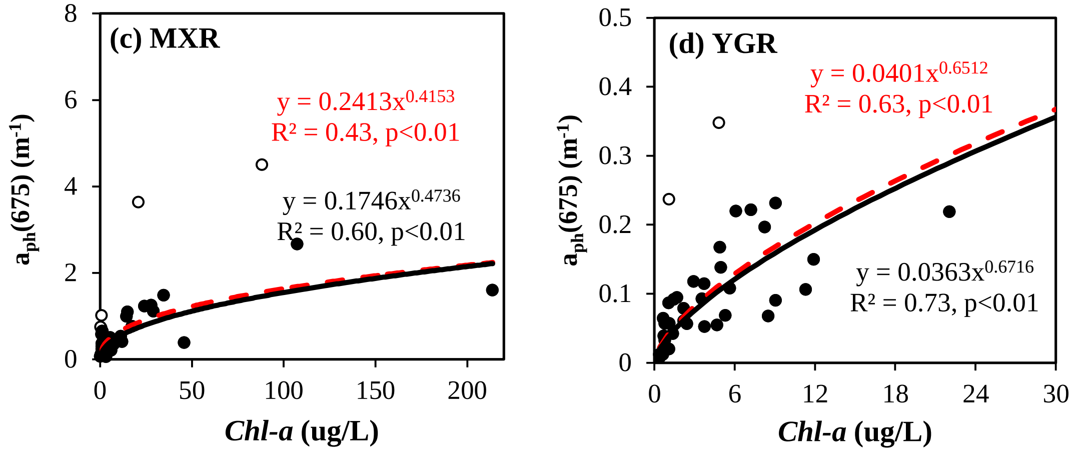

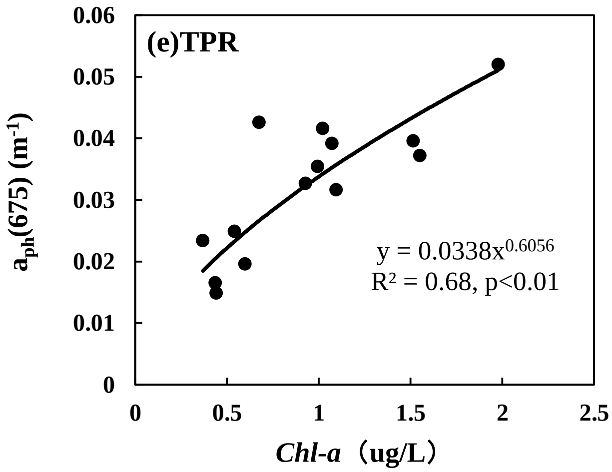

Fig. 3 The $a_{ph}(675)$ plotted against *Chl-a* concentration. (a) NLR; (b) ELR; (c)MXR; (d)YGR; (e)TPR.

Note: The hollow points represented the outliers in different regions; The dotted lines and black lines were the exponential models with outliers and without outliers respectively; The correlation equation with red was obtained including outliers; The correlation equation with black was obtained for eliminating the outliers.

3.3 NAP Absorption

For all the reservoirs investigated, the absorption coefficients for non-algal particle ($a_{NAP}(440)$) had a mean value of 1.42 m^{-1}. The non-algal particle absorption coefficient values showed an increasing trend for reservoirs with oligotrophic, mesotrophic to hyper-eutrophic states (Fig. S2). The mean $a^*_{NAP}(440)$ ranged from 0.021 to 0.43 m^2/g for various regions and trophic states was shown in Fig S3. There were significant differences between YGR and MXR (TPR) for $a^*_{NAP}(440)$. Significant but not so strong relations ($p<0.01$, $R^{2:}$ 0.35-0.66) were found between a_{NAP} and MSS in different regions (Fig.4). The mean S_{NAP} was 0.009, 0.015, 0.011, 0.016 and 0.021 um^{-1} for NLR, ELR, MXR, TPR and YGR respectively.

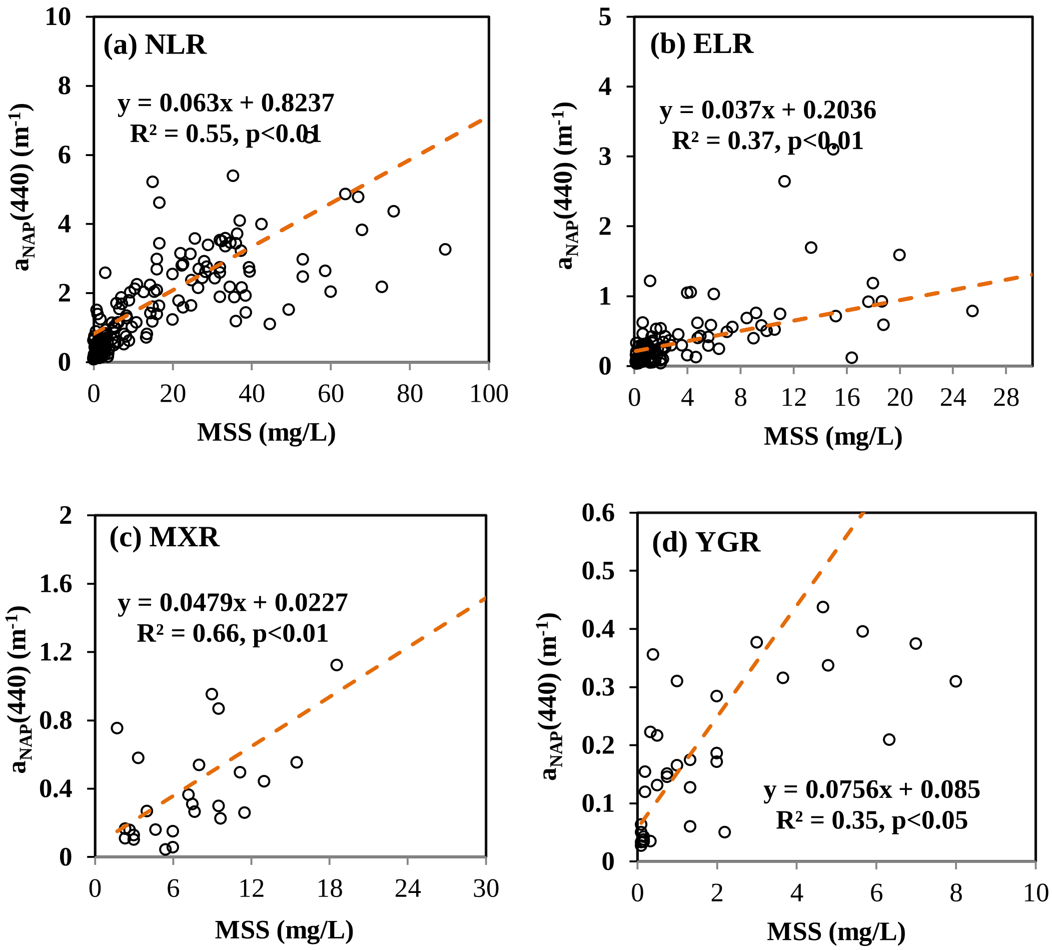

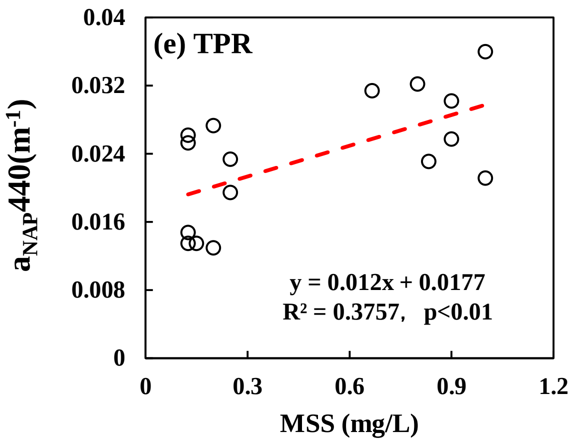

Fig. 4 Correlation between NAP absorption and MSS for lake regions, (a) NLR; (b) ELR; (c)MXR; (d)YGR; (e)TPR.

3.4 CDOM absorption

The CDOM absorption at 355 nm ranged from 0.34 to 12.11 m^{-1}, and the CDOM absorption at 440 nm ranged from 0.15 to 1.90 m^{-1} (Fig. 5). There was significant difference ($p<0.01$) among reservoirs of different trophic states within the same region with respect to CDOM absorption at 355nm. Within a region, the mean value of $a_{CDOM}(355)$ and $a_{CDOM}(440)$ for the reservoirs significantly increased with trophic state ($p<0.05$). The S_{CDOM}280-400 ranged from 10.99 to 25.47 μm^{-1}, with a mean value of 19.26 μm^{-1} (Fig.6). A decreasing trend for $S_{280\text{-}400}$ and $S_{275\text{-}295}$ was also observed with the increasing of trophic states (Fig.6). The mean a^*_{CDOM} for all reservoirs ranged from 0.14 to 0.92 L mg/m (Fig. S4). With the increasing of trophic states, the a^*_{CDOM} increased significantly ($p<0.05$). The relationships between $a^*_{CDOM}(355)$ and $S_{280\text{-}400}$ was significant ($p<0.01$) (Fig. S5) and the correlations between CDOM absorption coefficients ($a_{CDOM}(440)$ and $a_{CDOM}(355)$) and $S_{275\text{-}295}$ for various trophic states and regions were significant as well ($p<0.01$) (Table S2).

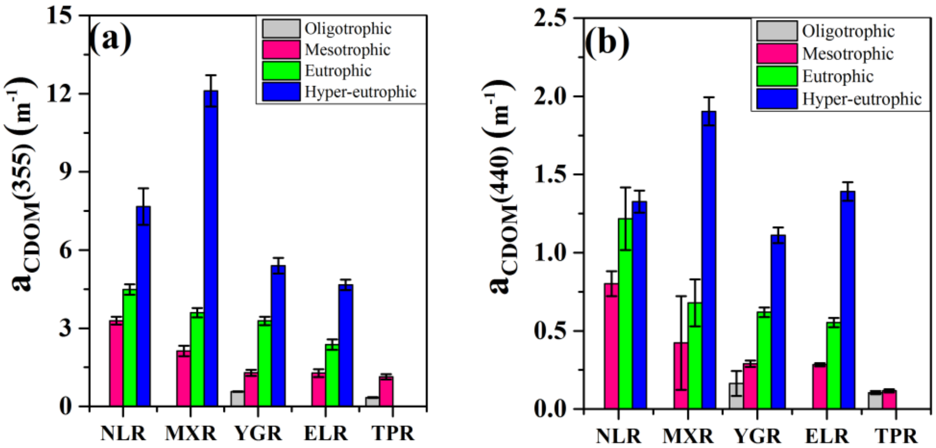

Fig.5 The comparisons of CDOM absorption at (a) 355nm, and (b) 440nm in different regions concerning with various trophic states.

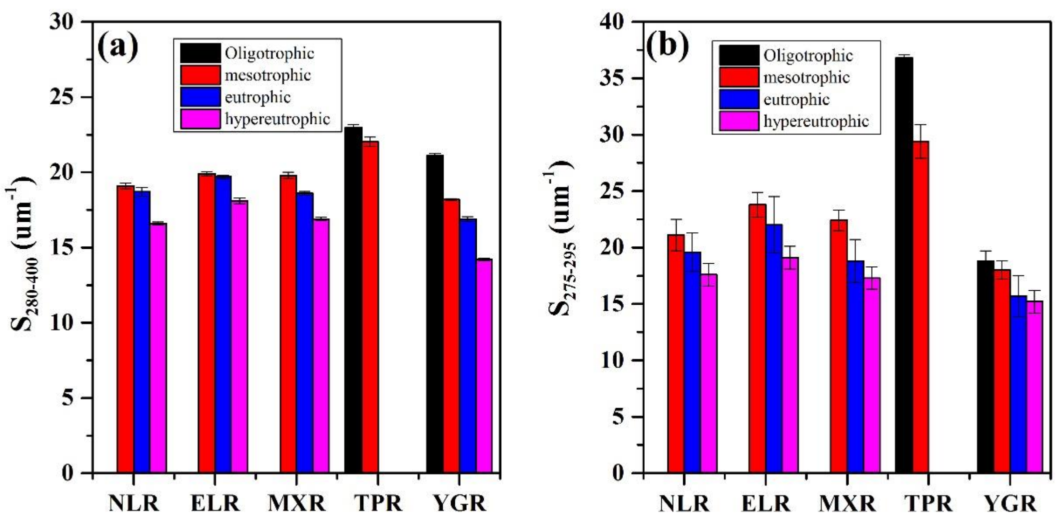

Fig. 6 Distribution of CDOM absorption spectral slopes with different wavelength ranges, (a) S_{CDOM}280-400, and (b) S_{CDOM}275-295 in different lake regions.

3.5 Total non-water absorption budget

The absorption of NAP in the NLR and MXR regions generally contributed the most to the total absorption between 400 and 550 nm while phytoplankton absorption was generally stronger than CDOM absorption in the MXR region (Fig. S6). For reservoirs in the ELR region, phytoplankton absorption dominated in the 400-700 nm spectral region. In the YGR region, the contribution of CDOM absorption was significantly higher than that of other OAC constituents given that these reservoirs had low eutrophic states. Fig.7 showed that the non-water absorption budget from our data as triangular diagrams in different hydrological regions and trophic states at 380 nm, 440 nm and 510 nm wavelength. The relative absorption ratios for OACs at 440 nm for various trophic gradients and hydrological regions was shown in Table S3. And the result of k-means clustering analysis on non-water absorption budget showed that the dominant water types was various among regions and trophic states (Table S4 and S5). With increased trophic state, the relative absorption ratios of phytoplankton absorption and NAP absorption increased while the ratios of CDOM absorption significantly decreased ($p<0.05$).

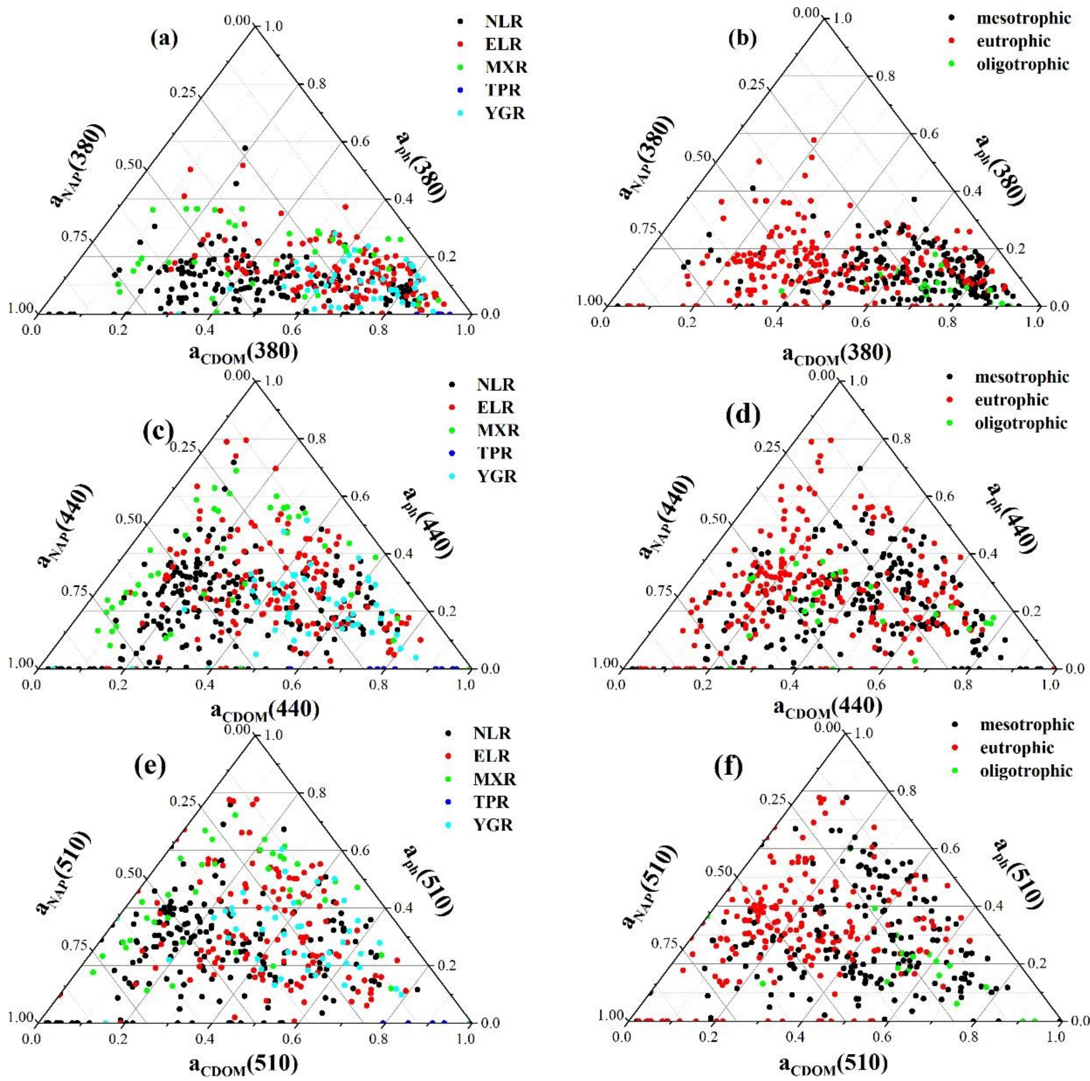

Fig.7 The relative contributions of CDOM, phytoplankton and non-algal particles to total non-water light absorption at 380 nm in different regions(a), and various trophic states(b); at 440 nm in different regions(c), and various trophic states(d); at 510 nm in different regions(e), and various trophic states(f).

3.6 Hydrological and water quality parameters for absorption properties

The influencing factors for the relative proportion of OACs absorption at 440nm in reservoirs including the hydrological factors and water quality factors were analyzed with multiple regression using SPSS 22.0 (Table 3). There are no correlations between absorption properties and temperatures ($p>0.05$) as our sampling fieldtrips were conducted in the autumn without obvious seasonal variability. The CDOM proportion was positively related to inactive storage (standardized Beta=0.437), DOC (standardized Beta=0.208) and was negatively related to TSM (standardized Beta=-0.429) ($p<0.005$). The TSM concentration (standardized Beta=0.472) and total storage (standardized Beta=-0.325) were significantly contributed to NAP absorption proportion positively and negatively. The phytoplankton absorption proportion was only related to water quality parameters such as *Chla* (standardized Beta=0.802) and TP (standardized Beta=0.356).

Table 3 The factors affecting OACs absorption proportion with multiple regressions

Types	Factors	Standardized Coefficients (Beta)	t	Significance
CDOM	Constant		13.778	0.000
	Inactive storage	0.437	3.302	0.002
	TSM	-0.429	-3.237	0.003
	DOC	0.208	2.327	0.025
NAP	Constant		12.532	0.000
	TSM	0.472	3.403	0.002
	Total storage	-0.325	-2.344	0.025
Phytoplankton	Constant		2.137	0.038
	Chla	0.802	9.118	0.000
	TP	0.356	2.753	0.010

4 Discussion

4.1 Phytoplankton absorption based on regions and trophic status

The variations of phytoplankton absorption are affected by the size composition variation of phytoplankton which can often be related to local eutrophic state (Brito et al., 2015; Le et al., 2013) and geographical settings (Mao et al., 2018), and the climatic conditions could affect the frequency of algal blooms and the spatial and vertical variations of *Chla*, and the wind-driven waves affect the bottom re-suspension and change the concentration of OACs (Xue et al., 2017). The lowest values for phytoplankton absorption coefficients were recorded in the YGR region mainly due to the low concentration of *Chla* and the relative oligotrophic state of reservoirs in this region (Astoreca et al., 2012). Conversely, the high concentration of *Chla* in the ELR region and the high trophic state of reservoirs in the MXR region indicated that reservoirs in these regions provided a suitable environment for phytoplankton growth, thus accounting for the high absorption coefficients recorded in reservoirs from these regions (Le et al., 2009). Although reservoirs in the NLR region were mostly eutrophic, relatively high TSM amounts were measured probably a consequence of strong spring winds causing the re-suspension of particulate matter (Li et al., 2015).

The variability in a^*_{ph} within a region indicated a change in pigment composition (Xue et al., 2017). Comparing mean a^*_{ph} for the ELR and NLR regions, the higher *Chla* concentration in ELR and NLR can be attributed to higher concentration of intracellular pigments or cell aggregation (Shi et al., 2013), and thus could account for the lower $a^*_{ph}(\lambda)$ values in these regions. Due to its design (reservoirs divided into regions and trophic state) and its geographical scope, results of our study should capture variability in geographical conditions and contribute to improvement in the accuracy of water quality optical models (Shi et al., 2019c), implying a challenge for parameterization of bio-optical algorithms for different regions (Cao et al., 2015; Shi et al, 2013).

4.2 Non-algal particle absorption based on regions and trophic status

In the present study, the fact that $a^*_{NAP}(440)$ decreased with increasing eutrophication across the five regions (Fig S3)would indicate that the level of eutrophication may affect the distribution of both organic and inorganic particles, and that more inorganic matter is imported into aquatic systems with increased trophic state (Babin et al., 2003). It has further been proposed that a lower S_{NAP} corresponds to mineral-dominated waters (Babin et al., 2003). In the present study, the highest S_{NAP} values were observed in the YGR region, which was companied with the weakest correlation between NAP absorption and MSS. The relative low S_{NAP} values in the MXR and NLR regions indicate that the NAP absorption of water reservoirs in these three regions was dominated by mineral matter. This is in good agreement with the strong correlation between NAP and MSS for the MXR and NLR regions. Despite being dominated by inorganic suspended matter, the regional variation in NAP absorption coefficient could probably be due to variation in the composition and size of inorganic particles (Astoreca et al., 2012). The variation in TSM concentration in reservoirs across the five regions could be associated with many factors; geographical characteristics and land-use are important contributing factors to the delivery of terrestrially-derived particles into water reservoirs (Wen et al, 2016). The trophic state of reservoirs could also affect phytoplankton production, microbial activity and degradation process, whereas the delivery of inorganic particles could translate into increase TSM concentration but also the release of particle-bound nutrients which in turn could lead to increased autochthonous production and *Chla* concentration (Astoreca et al., 2012). The complex interrelations between *Chla* and TSM concentration could have variable effects on light absorption. Climatic conditions, such as strong winds, were reported by Wen et al. (2016) to contribute to the re-suspension of bottom sediments in shallow water in the MXR region, resulting in particle absorption.

4.3 CDOM absorptions based on regions and trophic status

The variations of $S_{280\text{-}400}$ for different regions indicated the changes of aromaticity with humic acids, and fulvic acids (Niu et al., 2014). The S_{CDOM} values found in this study fell within the range of previous studies (Song et al., 2010; Niu et al., 2014), yet were higher than results from Lake Erie and Lake Qinghai (Zhou et al., 2005). The highest mean $S_{280\text{-}400}$ value (22.97 μm^{-1}) was recorded in Yamdrok Lake (TPR). As previously noted by Nima et al. (2016), high altitude, strong solar irradiance, low trophic states and climatic conditions can decrease phytoplankton activity, and lead to photo-bleaching and photo-induced degradation organic matters of reservoirs. In contrast, the lowest mean S value (16.9 μm^{-1}) was recorded in eutrophic reservoirs in the YGR region, indicating a dominance of aromatic materials likely from terrestrial sources (Cory et al., 2007). Climatic conditions in the YGR region (mean temperature of 17 °C and abundant precipitation; Liu et al., 2013), were conducive to degradation of plant detritus, the formation of aromatic humic materials and their transport to aquatic systems in the region (Sun et al., 1997).

Also, the negatively significant correlations between $a^*_{CDOM}(355)$ and $S_{280\text{-}400}$ were observed for all samples ($p<0.05$) (Fig.S5) which indicated the composition of CDOM would determine the degree of DOM color. The higher $a^*_{CDOM}(355)$ with increased trophic state in our study indicated the production of fresh DOM with short water retention time and more inputs from the surrounding catchments. Meanwhile, the lower $a^*_{CDOM}(355)$ and higher S in oligotrophic states and higher suggested more DOM age and the exposure to photo-chemical degradation process. The differences of correlation coefficients among various regions indicated the changes of CDOM composition and the degree of photo-degradation which was due to the content of lignin and the exposure to sunlight (Boyle et al. 2009, Organelli et al., 2014). With the increasing of trophic states, the inverse relationships indicated the increasing of allochothonous CDOM and the decreasing of photo-degradation process for mesotrophic reservoirs, while for the eutrophic states, both terrestrial DOM inputs and the strong microbial activities contributed to the complex trophic states.

4.4 Dominant optical absorptions and regulating factors for management

According to the optical classification of surface waters (based on relative contribution to the total absorption coefficients of OACs) (Prieur and Sathyendranath, 1981), in terms of trophic state, the proportion of CDOM absorption decreases while the ratio of NAP absorption to phytoplankton absorption increases, indicating that CDOM absorption is predominant in oligotrophic reservoirs while the NAP absorption is predominant in eutrophic waters. Thus, the reservoirs in the YGR and TPR regions can be classified into the “CDOM-type” whilst the majority of the reservoirs in the MXR and NLR regions can be classified as the “NAP-type”, ELR is calssified into “phytoplankton-type” according to the relative contribution to the total absorption coefficients of OACs.

The multiple regressions for relative OACs absorption proportions at 440nm based on hydrological and water quality factors (Table 3) indicated that the hydrological management and environmental protection for reservoirs would adjust the water optical absorption characteristics to some extent. The proportion of CDOM in reservoirs was related by inactive storage capacity, TSM and DOC. This was due to the increasing inactive storage capacity would extend the hydraulic retention time, and the decreasing of TSM concentration would relatively decrease the proportion of NAP absorption and increase the relative proportion of CDOM and phytoplankton absorption. The increasing of total storage would introduce lots of sediments and terrestrial input of solid matter which contributed to the accumulation of non-algal particles and the increasing proportion of NAP absorption. For phytoplankton absorption proportion, it was only closed to the water quality parameters including *Chla* and TP rather than other hydrological conditions.

Our results demonstrated the variation of the dominant absorption agent in different hydrological regions and trophic states and offered the detailed regulation conditions with hydrological and water chemical parameters to control the optical absorption characteristics (Shi et al., 2013). Also, the specific absorption coefficient for a given OAC should be different when bio-optical models are developed for remotely monitoring water quality constituents of reservoirs across China.

5 Conclusions

This study represents a systematic investigation of the variability of absorption properties of OACs in inland waters. The variation of sources and composition of OACs would affect the correlations between optical absorption parameters and relative water chemical parameters which is primary for remote monitoring of water quality in reservoirs for further study. It provides unique insights into the factors controlling that variability and requires for the parameterization of optical models in different regions. In addition, the differences of optical absorption characteristics in various regions which will help us to establish the more accurate remote sensing models of quasianalytical algorithm in different regions with remote sensing data for next step. The well understanding of spatial variations of IOPs are needed to meet the challenges to the variations of regional bio-optical modelling and water-quality parameter remote sensing algorithm parameterization and performance. Moreover, the good and significant relationships between the optical absorption characteristics and water quality parameters would provide more potential ways to calibrate the water quality parameters' monitoring models indirectly in future studies. It provides a simple outline for the classification of optically-complex waters, and therefore contribute to a new stage in the development of water type-specific algorithms.

Acknowledgments

The authors declare no conflicts of interest. The authors would like to thank the National Key Research and Development Project of China (2019YFC0409105), the Natural Science Foundation of China (No.41701423, No. 41730104, No. 42001311), the Project funded by China Postdoctoral Science Foundation (2020M681057) and the Outstanding Young Scientist Foundation of Institute of Northeast Geography and Agroecology (IGA) granted to Dr. Zhidan Wen. Youth Innovation Promotion association of Chinese academy of Sciences (2020234). The Special Research Assistant Funding Program of Chinese Academy of Sciences granted to Dr. Yingxin Shang. Thanks are also extended to all the staff and students for their efforts in field data collection and laboratory analysis.

References

Aizaki, M., (1981). Application of modified Carlson's trophic state index to Japanese lakes and its relationships to other parameters related to trophic state (in Japanese with English summary). Res Rep Natl Inst Environ Stud Jpn, 23, 13-31.

Astoreca, R., Doxaran, D. A. V. I. D., Ruddick, K., Rousseau, V., & Lancelot, C., (2012). Influence of suspended particle concentration, composition and size on the variability of inherent optical properties of the Southern North Sea. Continental Shelf Research, 35, 117-128.

Babin M., & Stramski, B. D. (2004). Variations in the mass-specific absorption coefficient of mineral particles suspended in water. Limnology and Oceanography, 49(3), 756-767.

Babin, M., Stramski, D., Ferrari, G. M., Claustre, H., Bricaud, A., Obolensky, G., & Hoepffner, N., (2003). Variations in the light absorption coefficients of phytoplankton, nonalgal particles, and dissolved organic matter in coastal waters around Europe. Journal of Geophysical Research: Oceans, 108(C7).

Binding, C. E., Bowers, D. G., & Mitchelson-Jacob, E. G. (2005). Estimating suspended sediment concentrations from ocean colour observations in moderately turbid waters; the impact of variable particle scattering properties. Remote Sensing of Environment, 94, 373−383.

Binding, C. E., J. H. Jerome, R. P. Bukata, & W. G. Booty (2008), Spectral absorption properties of dissolved and particulate matter in Lake Erie, Remote Sensing of Environment., 112, 1702–1711.

Boyle, E. S., Guerriero, N., Thiallet, A, Vecchio, R. D. & Blough, N. V.(2009). Optical properties of humic substances and cdom: relation to structure. Environmental ence & Technology, 43(7), 2262-2268.

Brezonik, P.L., Olmanson, L.G., Finlay, J.C., & Bauer,M.E. (2015). Factors affecting the measurement of CDOM by remote sensing of optically complex inland waters. Remote Sensing of Environment, 157, 199–215.

Bricaud, A. , Babin, M. , Morel, A. , & Claustre, H. . (1995). Variability in the chlorophyll-specific absorption coefficients of natural phytoplankton: analysis and parameterization. Journal of Geophysical Research Oceans, 100(C7), 13321-13332.

Bricaud, A., M. Babin, H. Claustre, J. Ras, & F. Tieche, (2010), Light absorption properties and absorption budget of Southeast Pacific waters, Journal of Geophysical Research Oceans, 115(115), 488-507.

Brito, A.C., Sá, C., Brotas, V., Brewin, R.J.W., Silva, T., Vitorino, J., Platt, T., & Sathyendranath, S., (2015). Effect of phytoplankton size classes on bio-optical properties of phytoplankton in the Western Iberian coast: application of models. Remote Sensing of Environment. 156, 537–550.

Cao W.，Yang Y.，Liu S., Xu X.Q., Yang D. T., & Zhang J. L., (2015). Spectral absorption coefficient of phytoplankton and its relation to chlorophyll a and remote sensing reflectance in coastal waters of southern China． Progress in Natural Science，2005, 15(4) : 342-350．

Ciotti, U. M. , Lewis, M. R. , & Cullen, J. J. (2002). Assessment of the relationships between dominant cell size in natural phytoplankton communities and the spectral shape of the absorption coefficient. Limnology and Oceanography, 47(2), 404-417.

Cory, R. M., McKnight, D. M., Chin, Y. P., Miller, P., & Jaros, C. L. (2007). Chemical characteristics of fulvic acids from Arctic surface waters: Microbial contributions and photochemical transformations. Journal of Geophysical Research: Biogeosciences, 112(G4).

Gholizadeh, M. H., Melesse, A. M., & Reddi, L. N. (2016). A Comprehensive Review on Water Quality Parameters Estimation Using Remote Sensing Techniques. Sensors, 16(8).

Helms, J. R., Aron, S., Ritchie, J. D., Minor, E. C., Kieber, D. J., & Kenneth, M. (2008). Absorption spectral slopes and slope ratios as indicators of molecular weight, source, and photobleaching of chromophoric dissolved organic matter. Limnology and Oceanography, 53, 955–969.

Jones, S. E., Newton, R. J., & McMahon, K. D., (2009). Evidence for structuring of bacterial community composition by organic carbon source in temperate lakes. Environmental microbiology,11(9), 2463-2472.

Le, C. F., Li Y. M., Zha Y., & Sun D. Y. (2009). Specific absorption coefficient and the phytoplankton package effect in Lake Taihu, China, Hydrobiologia, 619, 27–37.

Le, C., Hu, C., English, D., Cannizzaro, J., Chen, Z., Kovach, C., Anastasiou, C.J., Zhao, J., Carder, K.L., (2013). Inherent and apparent optical properties of the complex estuarine waters of Tampa Bay: what controls light? Estuarine Coastal and Shelf Science,117, 54–69.

Li, S. , Zhang, J. , Guo, E. , Zhang, F. , Ma, Q. , & Mu, G. . (2017). Dynamics and ecological risk assessment of chromophoric dissolved organic matter in the yinma river watershed: rivers, reservoirs, and urban waters. Environmental Research, 158(oct.), 245.

Li S. J., Song K. S., Wen Z. D,, Zhao Y., Shao T. T., Mu G. Y., & Guan Y., (2015). Absorption characteristics of praticulates and CDOM in spring in Lake Xingkai. Journal of Lake Sciences, 27(5):941-952.

Li, Y., Wang, Q., Wu, C., & Zhao, S., (2012). Estimation of chlorophyll a concentration using nir/red bands of meris and classification procedure in inland turbid water. IEEE Transactions on Geoscience & Remote Sensing, 50(3), 988-997.

Liu, J., Sun, D., Zhang, Y., & Li, Y., (2013). Pre-classification improves relationships between water clarity, light attenuation, and suspended particulates in turbid inland waters. Hydrobiologia, 711(1), 71-86.

Lyu, L., Wen, Z., Jacinthe, P. A. , Shang, Y. , Zhang, N. , & Liu, G. (2020). Absorption characteristics of cdom in treated and non-treated urban lakes in changchun, china. Environmental research, 182, 109084.1-109084.13.

Mao, D.H., Luo, L., Wang, Z.M., Wilson, M.C., Zeng, Y., Wu, B.F., Wu, J.G., (2018). Conversions between natural wetlands and farmland in China: a multiscale geospatial analysis. Science of the Total Environment, 634: 550-560.

Matsuoka, A., Hill, V., Huot, Y., Babin, M., & Bricaud, A., (2011). Seasonal variability in the light absorption properties of western arctic waters: parameterization of the individual components of absorption for ocean color applications. Journal of Geophysical Research Atmospheres, 116, 434-441.

Mitchel, B. G., Kahru, M., Wieland, J., & Stramska, M., (2002). Determination of spectral absorption coefficients of particles, dissolved material and phytoplankton for discrete water samples. Ocean optics protocols for satellite ocean colour sensor validation, Revision 4, Volume IV: Inherent optical properties: Instruments, characterizations, field measurements and data analysis protocols. Goddard Space Flight Center Technical Memorandum 2003-01674-0.

Naik, P., D'Sa, E. J., Gomes, H. d. R., Goés, J. I.. & Mouw, C. B., (2013). Light absorption properties of southeastern Bering Sea waters: analysis, parameterization and implications for remote sensing. Remote Sensing of Environment. 134, 120–134.

Nima, C., Hamre, B., Øyvind Frette, Erga, S. R., Chen, Y. C., & Zhao, L., (2016). Impact of particulate and dissolved material on light absorption properties in a high-altitude lake in tibet, china. Hydrobiologia, 768(1), 63-79.

Niu, C., Zhang, Y. L. , Zhu, G. W. , Wang, M. Z. & Liu, X. H. . (2014). Comparison of optical properties of dom and cdom in lake tianmuhu catchment. Research of Environmental ences, 27(9), 998-1007.

Organelli, E., Bricaud, A., Gentili, B., Antoine, D., Vellucci, V., (2016). Retrieval of colored detrital matter (CDM) light absorption coefficients in the Mediterranean Sea using field and satellite ocean color radiometry: evaluation of bio-optical inversion models. Remote Sensing of Environment. 186, 297–310.

Organelli, E., Bricaud, A., Antoine, D., & Matsuoka, A. , (2014). Seasonal dynamics of light absorption by chromophoric dissolved organic matter (CDOM) in the NW Mediterranean Sea (BOUSSOLE site), Deep-Sea Res. Pt. I, 91, 72–85.

Prieur, L. & Sathyendranath, S. (1981). An optical classification of coastal and oceanic waters based on the specific spectral absorption curves of phytoplankton pigments, dissolved organic matter, and other particulate materials, Limnology and Oceanography, 26, 671–689.

Shang,Y, Song, K, Jacinthe, P., Wen, Z.,(2019). Characterization of CDOM in reservoirs and its linkage to trophic status assessment across China using spectroscopic analysis. Journal of Hydrology, 576(1).

Shi, K., Li, Y., Li, L., & Lu, H., (2013). Absorption characteristics of optically complex inland waters: Implications for water optical classification. Journal of Geophysical Research: Biogeosciences, 118(2), 860-874.

Shi, K., Zhang, Y., Zhang, Y., Li, N., Qin, B., & Zhu, G. et al. (2019a). Phenology of phytoplankton blooms in a trophic lake observed from long-term modis data. Environmental Science & Technology, 53(5), 2324-2331.

Shi, K., Zhang, Y., Qin, B., & Zhou, B. (2019b). Remote sensing of cyanobacterial blooms in inland waters: present knowledge and future challenges. Science Bulletin, 20: 1540-1556

Shi, K., Zhang, Y., Song, K., Liu, M., & Qin, B. (2019c). A semi-analytical approach for remote sensing of trophic state in inland waters: bio-optical mechanism and application. Remote Sensing of Environment, 232, 111349.

Song K, Liu D, Li L, (2010). Spectral absorption properties of colored dissolved organic matter (CDOM) and total suspended matter (TSM) of inland waters[C]//SPIE Optical Engineering+ Applications. International Society for Optics and Photonics: 78110B-78110B-13.

Spyrakos, E., O"Donnell, R., Hunter, P. D., Miller, C., Scott, M., & Simis, S. G. H. , et al. (2017). Optical types of inland and coastal waters. Limnology and Oceanography.

Sun L, Perdue E M, Meyer J. L. & Weis J.(1997). Use of elemental composition to predict bioavailability of dissolved organic matter in a Georgia river. Limnology and Oceanography, 42: 714-721.

Sun, D., Li, Y., Wang, Q., Le, C., Lv, H., & Huang, C., (2012). Specific inherent optical quantities of complex turbid inland waters, from the perspective of water classification. Photochemical & Photobiological Sciences Official Journal of the European Photochemistry Association & the European Society for

Photobiology, 11(8), 1299–1312.

Tilstone, G. H., Peters, S. W. M., Woerd, H. J. V. D., Eleveld, M. A., Ruddick, K., & Schönfeld, W., (2012). Variability in specific-absorption properties and their use in a semi-analytical ocean colour algorithm for meris in north sea and western english channel coastal waters. Remote Sensing of Environment, 118(9), 320-338.

Vantrepotte, V., Loisel, H., Dessailly, D., & Mériaux, X., (2012). Optical classification of contrasted coastal waters. Remote Sensing of Environment, 123(8), 306-323.

Wan, W. , Zhang, Y. , Cheng, G. , Li, X. , & He, D. . (2020). Dredging mitigates cyanobacterial bloom in eutrophic lake nanhu: shifts in associations between the bacterioplankton community and sediment biogeochemistry. Environmental Research, 188.

Wen, Z. D., Song, K. S., Zhao, Y., Du, J., & Ma, J. H., (2016). Influence of environmental factors on spectral characteristics of chromophoric dissolved organic matter (CDOM) in Inner Mongolia Plateau, China. Hydrology and Earth System Sciences, 20(2), 787-801. doi: 10.5194/hess-20-787-2016

Wu, G., Cui, L., Duan, H., Fei, T., & Liu, Y.,(2011). Absorption and backscattering coefficients and their relations to water constituents of poyang lake, china. Applied Optics, 50(34), 6358-68.

Xue, K., Zhang, Y., Duan, H., & Ma, R. (2017). Variability of light absorption properties in optically complex inland waters of Lake Chaohu, China. Journal of Great Lakes Research, 43(1), 17-31.

Zhang, Y. L., Y. Yin, E. L. Zhang, G. W. Zhu, M. L. Liu, L. Q. Feng, B. Q. Qin & X. H. Liu, (2011). Spectral attenuation of ultraviolet and visible radiation in lakes in the Yunnan Plateau, and the middle and lower reaches of the Yangtze River, China. Photochemical and Photobiological Sciences, 10, 469–482.

Zhang, Y. , Zhou, Y. , Shi, K. , Qin, B. , Yao, X. , & Zhang, Y. . (2018). Optical properties and composition changes in chromophoric dissolved organic matter along trophic gradients: implications for monitoring and assessing lake eutrophication. Water Research, 131, 255-263.

Zhao, Y. H., Deng X. Z., Zhan, J. Y., Xi, B. D. & Lu, Q. (2010). Progress on preventing and controlling strategies of lake eutrophication in China. Environmental Science & Technology (China), 33, 92-98.

Zhao, Y, Song, K. , Wen, Z. , Fang, C. , Shang, Y. , & Lv, L. (2017). Evaluation of cdom sources and their links with water quality in the lakes of northeast china using fluorescence spectroscopy. Journal of Hydrology, 550, 80-91.

Zhou. H.L, Zhu. J. H., Li. T. J., & Wang. X. Y.,(2005). The analysis of water color absorption spectral characteristics in Qinghai Lake. Ocean Technology, 55-58